Energy flux into a fluidized granular medium at a vibrating wall

Sean McNamara* and Jean-Louis Barrat
Département de Physique des Matériaux, Université Claude Bernard and CNRS, 69622 Villeurbanne Cedex, France
(Received 25 July 1996)

We study the power input of a vibrating wall into a fluidized granular medium, using event-driven simulations of a model granular system. The system consists of inelastic hard disks contained between a stationary and a vibrating elastic wall, in the absence of gravity. Two scaling relations for the power input are found, both involving the pressure. The transition between the two occurs when waves generated at the moving wall can propagate across the system. Choosing an appropriate wave form for the vibrating wall removes one of these scalings and renders the second very simple. [S1063-651X(97)02405-7]

PACS number(s): 05.60.+w, 46.10.+z, 05.70.Ln, 47.11.+j

One of the essential differences between fluidized granular systems and usual gases is that sustaining a fluidized state necessitates a continuous input of energy into the system since the particle kinetic energy is dissipated during the collisions. Experimentally, this is often achieved by using a vibrating piston. The nature of the energy exchange between the vibrating piston and the fluidized granular medium, however, does not appear to have been studied in great detail. In most cases, it is assumed that the vibrating wall imposes a ''granular temperature'' of the particles that corresponds to its mean-squared velocity. The purpose of this work is to achieve a more detailed understanding of this energy exchange by studying numerically and theoretically a particularly simple case. The system we consider [Fig. 1(a)] is a two-dimensional fluid of inelastic hard disks, contained between two walls in the y direction and with periodic boundary conditions in the x direction. The moving wall is, at its lowest point, at $y=0$, while a stationary wall limits the system at $y=H$. For the sake of simplicity, we have chosen to treat the wall-particle collisions as elastic and to set the gravity force equal to zero. Hence the system can be entirely characterized by a small number of dimensionless parameters. These parameters are the ratios of the system sizes H (in the y direction) and L (in the x direction) to the particle radius a, the density measured by the area fraction $N\pi a^2/LH$ (N is the number of particles), the amplitude of vibration A of the moving wall, measured in units of a, and the restitution coefficient $r<1$. [In the center-of-mass frame of two colliding particles $v_n'=-rv_n$, where v_n (v_n') is the normal component of the particles' velocity before (after) the collision.] Finally, the problem is completely defined by specifying the wave form $\phi(t)$ of the wall vibration. Note that τ, the period of this wave form, defines the time unit in the problem. There is a second time scale in the problem: t_{coll}, the time between collisions experienced by an average particle. But t_{coll} is not independent of τ; the ratio τ/t_{coll} is a function of the five dimensionless numbers given above. In the simulations considered here, $2\leqslant\tau/t_{\mathrm{coll}}\leqslant 40$. In Fig. 1(b) we show the two wave forms, labeled (A) and (B), used to drive the vibrating wall.

We note that the system studied in this paper is an externally driven version of the system considered in Refs. [1–3]. Despite its simplicity, this system was shown to display a nontrivial behavior even in the absence of external forcing, with the development of several instabilities during ''homogeneous cooling.'' Other instabilities, such as the formation of lateral structures in the x direction, could be expected in the forced case. Since our main object is the study of energy input at a local scale, we deliberately avoided such structures by using a relatively small system width $L/a=50$.

If we were to add gravity to the system studied in this paper, we would have the system studied in Refs. [4–8]. The most important results of this paper can be modified to include gravity, as we discuss at the end.

If we were to drive the system by imposing a ''granular

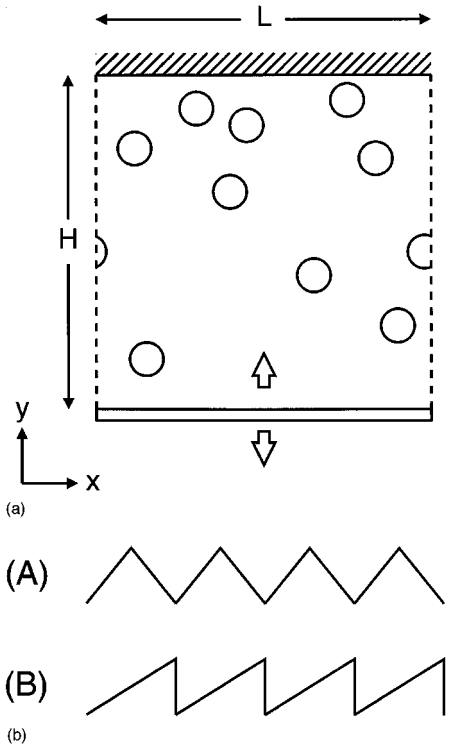

FIG. 1. (a) Sketch of the system studied. (b) Two wave forms used to drive the vibrating wall: the symmetric wave form (A) and the asymmetric wave form (B).

*Present address: ICA 1, Pfaffenwaldring 27, 70569 Stuttgart, Germany.

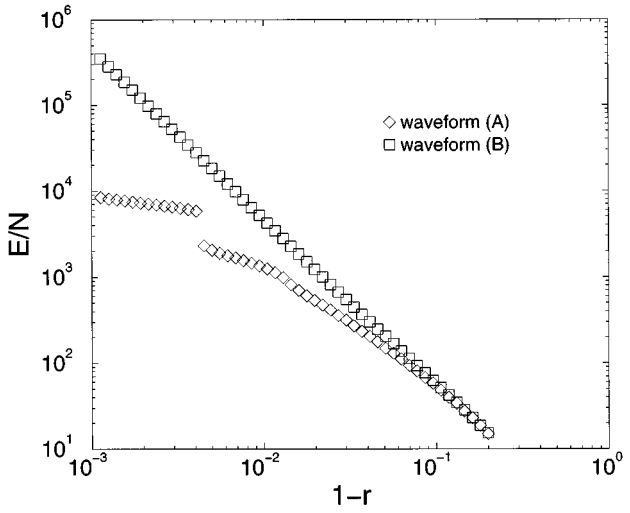

FIG. 2. Average energy per particle as a function of r, showing the effect of changing the wave form of the vibrating wall. The parameters of these simulations are $L=H=50a$, area fraction $N\pi a^2/LH=0.25$, wall velocity $V=8a/\tau$, and $0.8\leqslant r\leqslant 0.998\,866$. Energy is measured in units of ma^2/τ^2, where m is the mass of one particle.

temperature'' at one wall, we would have the system studied in Ref. [9]. A comparison of these two papers enables one to see the effects of the vibrating plate boundary condition. We also note that the focus of [9] is complementary to ours: They are concerned with the interior, whereas we concentrate on the boundaries.

Figure 2 shows that a detailed understanding of the particle-wall interaction is needed. When the wall is driven with the asymmetric wave form B, the relation between the average energy per particle E/N and the restitution coefficient obeys a simple power law $E/N\sim(1-r)^{-1.9\pm0.1}$. On the other hand, the symmetric wave form A generates much more complicated behavior. Since the only difference between these two curves is the wave form, their differences cannot be explained without understanding what happens at the vibrating boundary. This paper explains how the wave form causes the two different relations between E/N and r.

We begin by looking closely at what is happening inside the system. We show typical density and temperature profiles in Fig. 3, for a system driven by a symmetric wave form [type A in Fig. 1(b)]. The evolution of the profiles during the wall motion is also detailed in these figures. As the vibrated system is ''heated'' by the moving wall, an inhomogeneous density and temperature (temperature being understood here as kinetic energy per particle) profile develops. Far from the moving wall, the system is denser and cooler than close to it. The temperature profile clearly displays two different regions. In a region that extends over about half the height H of the box, a heat pulse generated at the vibrating wall propagates in the positive y direction. Farther away from the moving wall, the heat pulses are completely damped and the temperature is stationary. The ''boundary region'' for the temperature thus appears to be rather broad. The density profile also displays a (small) time-dependent component, indicating that the heat pulses are coupled to compression waves in the fluid. These heat and density waves can transport significant amounts of energy within the boundary region. This

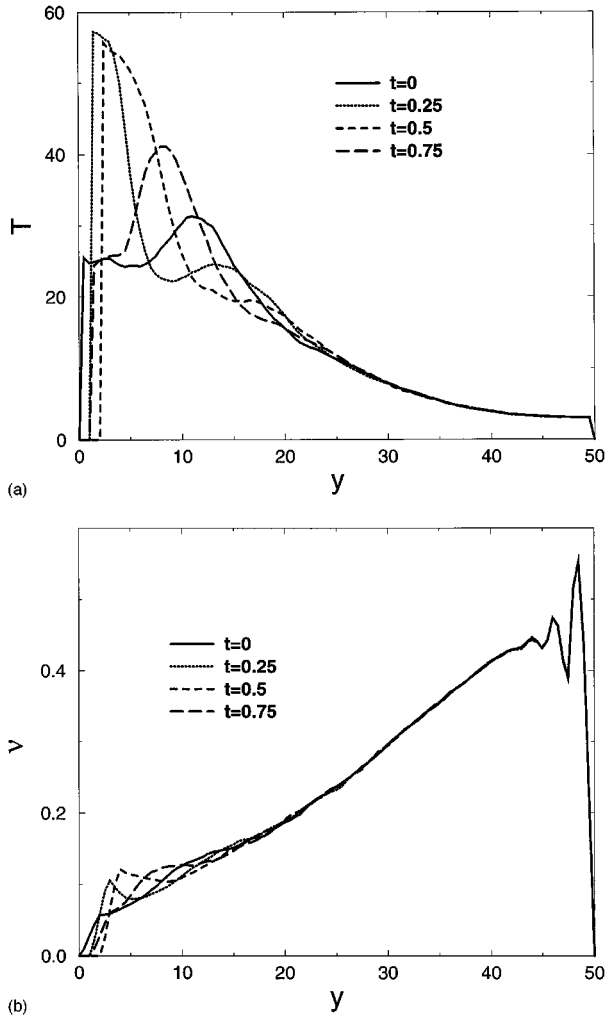

FIG. 3. Profiles of (a) temperature (energy per particle in units of ma^2/τ^2) and (b) density (measured by the local area fraction ν). The nondimensional parameters are $L=H=50a$, $r=0.95$, $N\pi a^2/LH=0.25$, $A=2a$, and the symmetric wave form. [There are about $N/(L/2a)\approx 8$ layers of particles.] For these values of the parameters, $\tau/t_{\rm coll}=3.39$. In each graph, there are four lines showing the field values at four times during the driving cycle. The wall is at its lowest point ($y=0$) at $t=0$ and at its highest point ($y=A=2$) at $t=0.5$. At $t=0.25$ ($t=0.75$), it is halfway between these extremes and ascending (descending). These profiles were made by averaging over 2000 cycles. In low-density regions, the fluctuations between one cycle and another are large. However, fluctuations between averages over many cycles are small, as shown by the smoothness of the curves.

is in conflict with the assumption that energy transport is dominated everywhere by conduction (for example, in [6]). We note that similar waves have been studied in shaken granular materials under gravity [7,8]. These waves resemble sound waves in a gas. However, their description in terms of a single ''temperature'' is not perfectly accurate. A more careful examination shows that the particles in these waves can be divided into two distinct populations with significantly different kinetic temperatures. One population is made up of rapidly moving particles that, having just encountered the moving wall, travel towards the stationary region, carrying the heat pulses. The other is a population of slowly mov-

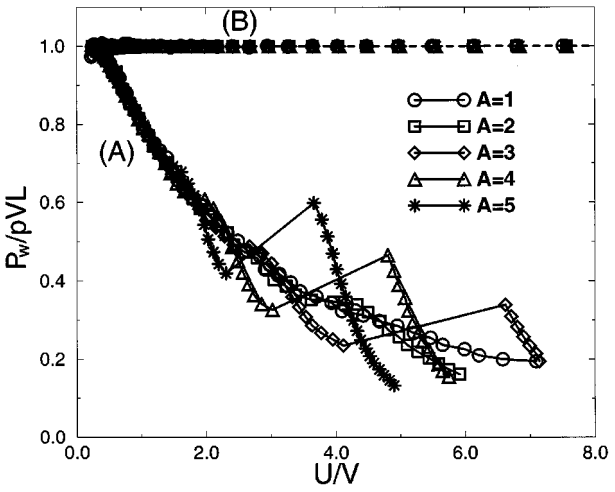

FIG. 4. Power input scaled as $P_w = pVLF(U/V)$. The points joined by the solid line and labeled (A) were generated by the symmetric wave form, those joined by the dashed line and labeled (B) by the asymmetric one. The parameters are $L = H = 50a$, $N\pi a^2 = 0.25$, $1 \leqslant A \leqslant 5$ (as indicated on the graph), and $0.8 \leqslant r \leqslant 0.998\,866$.

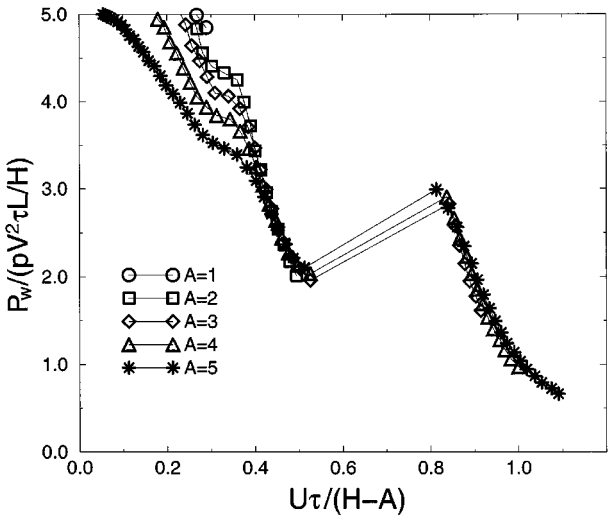

FIG. 5. Same data as the points joined by the solid line in Fig. 4 (symmetric wave form), but scaled with the second scaling presented in the text: $P_w = (pV^2 L\tau/H)G[U\tau/(H-A)]$. The points that disobey the previous scaling collapse onto a single curve. The gap at $0.5 \leqslant U/(H-A) \leqslant 0.8$ is caused by the resonance between the heat pulses and the vibrating wall. This gap corresponds to the discontinuities in Figs. 2 and 4.

ing particles emerging from the stationary region and traveling towards the moving wall.

We now seek a law giving the power injected by the wall P_w in terms of the kinetic pressure p (defined as the momentum transfer to the stationary wall per unit surface and time). Because of momentum conservation, the pressure on the vibrating wall must also be p, and dimensional reasoning suggests that the power input should be proportional to the force on the wall pL times the wall velocity V. For the asymmetric wave form B, this proportionality is indeed easily shown to hold as an equality. The argument is as follows. Collisions between the particles and the wall take place only when the wall is in its ascending phase. When such a collision takes place, the energy change and the momentum change of the particle are related by $\Delta E = V\Delta p_y$. Summing over all particles that hit the wall during a cycle shows that the average energy transfer per unit time will be equal to the wall velocity multiplied by the momentum transfer per unit time, i.e., $P_w = pVL$. This conclusion is extremely well borne out by the simulation results, as can be seen in Fig. 4.

The reasoning can be generalized to the case of other wave forms, e.g., A. In that case, the particles can either receive or lose energy as they hit the wall. If the arrival times of the particles at the vibrating wall are independent of the phase of the vibrating wall, then the probabilities of these two events will depend only on the ratio between velocity of the particles and the wall velocity V, so that we expect the power input to scale as $pVLF(U/V)$, where U is a velocity characteristic of the particles that hit the wall and F is a dimensionless function that will depend on the wave form and on the velocity distribution of the particles near the wall. In Fig. 4 this scaling relation was tested by plotting the power input as a function of the dimensionless variable U/V, where the typical particle speed U is estimated by the square root of the average energy per particle $(E/N)^{1/2}$ [10]. The unscaled values of P_w range over four orders of magnitude, so the success of the scaling is impressive. The scaling is very well obeyed except for the largest amplitudes of wall vibration, in which case it fails for small values of the rescaled power input P_w/pVL.

The failure of the scaling relationship for small P_w/pVL can be traced back to the extension of the boundary region over the whole simulation cell. As r increases towards 1, the pulses generated by the wall broaden and propagate further. Eventually, they reach the opposite wall, so that the stationary region no longer exists. The entire box is filled by a standing wave driven by the vibrating wall. The transition to this situation is observed for values of the restitution coefficient very close to one and for large vibration amplitudes and only in the case where the excitation is of the form A. When this transition takes place, the points in Fig. 4 leave the scaling curve, displaying a discontinuous and nonmonotonic behavior. The points leave the scaling curve because the arrival times of the particles at the moving wall are no longer independent of the phase of the wall vibration, so that the simple assumptions used in deriving the scaling relationship break down. Moreover, the nonmonotonic behavior is caused by resonances between the driving frequency and modes of the granular ''gas'' between the two plates. (The discontinuity occurs when the standing wave changes mode number.)

This physical picture suggests a second scaling relationship. In Fig. 5 we show that $P_w = (pV^2\tau L/H)G[U\tau/(H-A)]$, where G is another dimensionless function. (The inclusion of the period of the wall vibration τ is required dimensionally.) This second scaling is valid everywhere the first one fails. It can be understood by considering the heat pulses as sound waves in a gas, with grains playing the role of molecules. The wave speed scales as U, so $U\tau/(H-A)$ is the fraction of the box that a wave can travel during one period. For particular values of $U\tau/(H-A)$, resonance between the wall and the waves will occur. P_w will scale as $\hat{p}VL$, where $\hat{p}$ is the pressure amplitude of the wave. Examining the properties of sound waves in a compressible gas at

pressure p, we find that the pressure and velocity amplitudes are related by $\hat{p}=(k/\omega)p\hat{u}$, where $\hat{u}$ is the velocity amplitude, k is the wave number of the wave, and ω is its frequency. Setting $\hat{u}\sim V$, $k\sim H^{-1}$, and $\omega\sim\tau^{-1}$ gives the scaling in Fig. 5.

The resonance affects the power injected by the wall only for the symmetric wave form A, even though waves generated by the asymmetric wave form B can also propagate throughout the box at large A and r close to 1. The reason is that particles can either gain or lose energy with the symmetric wave form. Thus, shifting the arrival time of a large group of particles by half a period can change the sign of P_w. On the other hand, for the asymmetric wave form B, the amount of energy gained by the particles does not depend on the phase of the wall.

The transition between the two scalings occurs at the critical value $U\tau/(H-A)\approx 0.4$. Examination of simulations made with $30<H<100$ confirms that this critical value remains constant. At this time, we do not have a satisfying explanation for this critical value. Examination of temperature profiles confirm that the transition occurs when the wave propagates all the way through the system. However, an estimate based on the decay of the wave due to diffusion predicts the transition will occur at a critical value of $U^2\tau^2/lH\sim p\tau^2/H$ (l is the mean-free path), but this is not true.

The theoretical innovation of this paper is to consider the energy flux as a function of the pressure instead of the local granular temperature (as in [6]). It is this difference that distinguishes the scaling relations presented here from others in the literature.

We believe these results to be relevant to current experimental questions. First of all, an experimental version of this system will soon be studied in microgravity [11]. Second, these results can easily be extended to experiments done in gravity by realizing that conservation of momentum requires that the pressure (the time-averaged force on the bottom plate) be the weight of the granular material: $pL=Nmg$. Finally, this work suggests that using the wave form B (or an experimental approximation) may simplify results, leading to a better physical understanding of granular flows.

This work was supported by Grant No. 96/CNES/0367 from the Centre National d'Etudes Spatiales. S.M. benefited from a Region Rhones-Alpes visiting scientist position at the Pole Scientifique de Modélisation Numérique of ENS-Lyon.

[1] I. Goldhirsch and G. Zanetti, Phys. Rev. Lett. **70**, 1619 (1993).
[2] S. McNamara and W.R. Young, Phys. Rev. E **53**, 5089 (1996).
[3] P. Deltour and J.L. Barrat, J. Phys. (France) I **7**, 137 (1997).
[4] S. Warr, J. Huntley, and G. Jacques, Phys. Rev. E **52**, 5583 (1995).
[5] S. Luding, H. Herrman, and A. Blumen, Phys. Rev. E **50**, 3100 (1994).
[6] J. Lee, Physica A **219**, 305 (1995).
[7] J. Lee, Physica A **238**, 129 (1997).
[8] A. Goldshtein, M. Shapiro, L. Moldavsky, and M. Fichman, J. Fluid Mech. **287**, 349 (1995).
[9] E.L. Grossman, T. Zhou, and E. Ben-Naim, Phys. Rev. E **55**, 4200 (1997).
[10] In Fig. 4 we have estimated U with $U_{\rm sys}$, an average over all particles in the system, whereas P_w is determined only by $U_{\rm wall}$, the average particle speed at the wall. But when H and N are fixed, $U_{\rm sys}$ is related to $U_{\rm wall}$ by a fixed constant. Thus we can use $U_{\rm sys}$ (which is much easier to measure) in Fig. 4. However, when H or N is varied, the relation between $U_{\rm sys}$ and $U_{\rm wall}$ varies also and we must use $U_{\rm wall}$ to collapse the data onto a single curve.
[11] S. Fauve (private communication).